Brief communication

MOLECULAR METABOLISM

Role of mitochondrial uncoupling protein-2 (UCP2) in higher brain functions, neuronal plasticity and network oscillation

Gretchen Hermes [1,3], David Nagy [2,4], Michael Waterson [2,4], Attila Zsarnovszky [2,4], Luis Varela [2,4], Mihaly Hajos [2,4], Tamas L. Horvath [2,*]

ABSTRACT

Background/Purpose: Major psychiatric illnesses, affecting 36% of the world's population, are profound disorders of thought, mood and behavior associated with underlying impairments in synaptic plasticity and cellular resilience. Mitochondria support energy demanding processes like neural transmission and synaptogenesis and are thus points of broadening interest in the energetics underlying the neurobiology of mental illness. These experiments interrogated the importance of mitochondrial flexibility in behavior, synaptic and cortical activity in a mouse model.
Methods: We studied mice with ablated uncoupling protein-2 expression (UCP2 KO) and analyzed cellular, circuit and behavioral attributes of higher brain regions.
Results: We found that mitochondrial impairment induced by UCP2 ablation produces an anxiety prone, cognitively impaired behavioral phenotype. Further, NMDA receptor blockade in the UCP2 KO mouse model resulted in changes in synaptic plasticity, brain oscillatory and sensory gating activities.
Conclusions: We conclude that disruptions in mitochondrial function may play a critical role in pathophysiology of mental illness. Specifically, we have shown that NMDA driven behavioral, synaptic, and brain oscillatory functions are impaired in UCP2 knockout mice.

Keywords Mental illness; Mitochondria; Uncoupling proteins; Auditory gating; NMDA receptor antagonism; Behavioral phenotype

1. INTRODUCTION

Major psychiatric illnesses are profound disorders of thought and emotion, which are strongly associated with underlying impairments in synaptic plasticity and cellular resilience. Mitochondria support energy demanding processes like neural transmission, and synaptogenesis, and are thus promising points of broadening interest in the energetics underlying the neurobiology of mental illness [1]. A case report of patients with mitochondrial cytopathy documented that 54% of study participants had major depressive disorder (MDD), 17% bipolar disorder, 11% panic disorder and 60% reported a family history of psychiatric illness [2]. Evidence from functional assays, protein expression studies and linkage analyses, points to a specific role for mitochondria in psychotic illnesses [1]. Patients with bipolar disorder have been shown to have impaired brain energy metabolism and increased mitochondrial DNA mutations [1]. A recent report on major depressive disorder demonstrated significantly reduced mitochondrial energy production in neurons of patients compared to controls [3].

With this in mind, we turned to a genetic model in which mitochondrial responses to energy demands are impaired. The mouse model presented here includes a deletion of uncoupling protein 2 (UCP2), a mitochondrial membrane protein that separates oxidative phosphorylation from ATP synthesis via controlled proton re-entry into the mitochondrial matrix [4]. In neurons, sustained UCP2 mediated uncoupling leads to increased mitochondrial proliferation and greater ATP production, making neurons more adaptive to dynamic fluctuations in neuronal activity [4]. We have shown that in the absence of UCP2, neurons are less plastic in response to stress. The translational value of this line of inquiry is clear as UCP2 is widely distributed in the central nervous system of humans including in basal ganglia, hippocampus, and cortex. Early evidence of UCP2's potential importance for mental illness has been demonstrated through post-mortem studies of

[1]Yale School of Medicine, Department of Psychiatry, 300 George St., Suite 901, New Haven, CT 06511, USA [2]Yale School of Medicine, Section of Comparative Medicine, 310 Cedar St., BML 330, P.O. Box 208016, New Haven, CT 06520-8016, USA

[3] Tel.: +1 203 764 9131.
[4] Tel.: +1 203 785 2525.

*Corresponding author. Tel.: +1 203 785 2525.

E-mails: gretchen.hermes@yale.edu (G. Hermes), david.nagy@yale.edu (D. Nagy), mike.waterson@yale.edu (M. Waterson), zsarnovszky.attila@aotk.szie.hu (A. Zsarnovszky), luis.varela@yale.edu (L. Varela), mihaly.hajos@yale.edu (M. Hajos), tamas.horvath@yale.edu (T.L. Horvath).

Received March 8, 2016 • Revision received March 29, 2016 • Accepted April 1, 2016 • Available online 9 April 2016

http://dx.doi.org/10.1016/j.molmet.2016.04.002

patients with schizophrenia and bipolar disorder showing reduced mRNA expression of UCP2 in cortex [5].

In published preclinical studies, using an UCP2 +/+ mice, we demonstrated that voluntary exercise induced UCP2 mRNA expression and oxygen consumption in the hippocampus [6]. These changes in metabolic demands resulted in increased mitochondrial number and dendritic spine synapses. Importantly, these changes in plasticity, mitochondrial and synaptic, did not occur in UCP2 KO animals, a further confirmation of the important role of UCP2 in neuronal and mitochondrial flexibility [6]. At the outset of the current studies, we hypothesized that the importance of mitochondria may be particularly salient for the cortex, where sustained recurrent neuronal firing has particularly high metabolic demands. Inadequate metabolic resources in the UCP2 KO model over a sustained period of time potentially contribute to abnormalities in the dendritic tree, architectural changes that underlie the deteriorating long-term course of mental illness.

Here we use an UCP2 KO mouse model to probe the role of reduced mitochondrial function in measures relevant to mental illness—emotionality, cognition, and activity in response to NMDA receptor blockade (psychotomimetic), synaptic plasticity and brain oscillatory and sensory gating activities, these latter measures considered endophenotypes of mental illness.

2. MATERIALS AND METHODS

2.1. Animal subjects

The Institutional Animal Care and Use Committee of Yale University approved all experiments. Mice were kept under standard laboratory conditions with free access to standard chow food and water except during behavioral testing periods. The generation of ucp2$^{-/-}$ mice has been previously described [7]. Animals included in behavioral studies were between 3 and 5 months of age.

2.2. Behavioral assessments

A series of behavioral assessments was used to establish the behavioral phenotype of UCP2 KO mice and its relevance as a model for aspects of neuropsychiatric illness. All behavioral testing was done in the light phase.

2.2.1. Elevated plus maze (EPM)

The maze is elevated 50 cm from the floor and has four 16 cm × 5 cm arms. Two arms are enclosed by 12-cm walls and the other 2 arms have a 3-mm edge to prevent the animals from slipping off the maze. The maze is illuminated equally on all four arms. Mice were placed on an open arm facing away from the center and were allowed to explore the maze for 5 min. Behavioral performance was recorded by overhead camera equipment and Any-MAZE™ software. Animals were carefully monitored and observed throughout testing.

2.2.2. Tail suspension test (TST)

Mice were suspended from a metal hanger inside of a tail suspension chamber (PHM-300; MED Associates, Inc. [3]; St. Albans, VT) for five minutes. A load cell and amplifier (ENV-50TS; MA) interfaced with data collection software (SOF-821; MA) was used to measure activity with a lower threshold value set at 2. Time immobile was defined as any period below the lower threshold value. Mice were acclimated to the behavior room with white noise for at least one hour prior to testing, and all equipment were cleaned with 60% ethanol between mice.

2.2.3. Open field

The open field test apparatus was a square, polyurethane arena (36.5 cm × 36.5 cm × 30 cm, Plexiglas). The animal was placed in corner of the apparatus locomotion speed, distance traveled, entries into the central zone, and time spent in contact with the outer walls, were recorded for 5 min. Behavioral testing took place from 1000 to 1400 h (i.e. in the light phase of the light—dark cycle). The apparatus was cleaned with 10% ethanol after each animal exposure. ANY-Maze Software™ (Stoelting Company, Wood Dale, IL) was used to record and analyze behavioral data.

2.2.4. Lashley maze

The Lashley III maze is a complex task that can be solved by learning the correct sequence of right—left responses, or extra-maze cues, or both [8]. Each day, animals were moved to the behavior testing room for thirty minutes prior to testing to allow them to acclimate to the testing environment. At that time, food and water was removed from all home cages. At the beginning of maze testing, mice were placed in the start box. Recorded test time begins when the door of the start box is opened. A mouse is considered to enter a new zone or arm of the maze when its body has crossed into that area. The trial is completed when the mouse has completely entered the pseudo-home cage at the end of the maze. Testing is repeated, with one trial per testing day per animal, until all mice reach a learning criteria defined as two consecutive trials with zero or one errors or until 14 days have elapsed [9]. Using overhead camera equipment and Any-MAZE™ software, Lashley maze activity was recorded and analyzed.

2.2.5. Y-maze

Spatial memory was assessed using the two-trial Y-maze task previously developed to study memory and recognition in rats [10]. A single Y-maze was made of black Plexiglas and consisted of three arms with an angle of 120° between each of the two arms. Each arm was 8 cm × 30 cm × 15 cm (width × length × height). The three arms were randomly designated: start arm, in which the mouse started to explore (always open), novel arm, in which the mouse started to explore (always open), novel arm, which was blocked during the first trial but open during the second trial. The maze was placed on a flat surface within the behavioral testing room. Proximal visual cues (pictures within the arms of the apparatus) and distal visual cues (the configuration of the room, curtain, and wall art) remained constant throughout testing. The floor of the maze was covered with white chip bedding. Between each trial the apparatus was cleaned with 10% ethanol and new bedding was added. Behavioral testing took place from 1000 to 1400 h (i.e. in the light phase of the light—dark cycle). The Y-maze test consisted of two trials separated by an inter-trial interval (ITI) of 60 min to assess spatial memory. The first trial had a five-minute duration and allowed the mouse to freely explore only two arms (start arm and other arm) while the third arm was blocked. After a 60 min ITI, the second trial also of five minutes duration was conducted during which all three arms were accessible and novelty vs. familiarity was compared in all three arms. ANY-Maze Software™ (Stoelting Company, Wood Dale, IL) was used to record and analyze behavioral data.

2.3. Response to NMDA receptor antagonist (MK 801)

Mice from were brought from the animal colony to the behavioral testing room. They were first habituated to the testing room for thirty minutes and then habituated to recording chambers for two hours prior to challenge. These chambers were opaque plexi-glass chambers measuring 24 cm W × 20 cm H × 46 cm L with alpha-dri™ bedding in the floor of the testing chambers. At the end of the habituation period, mice received an injection of the NMDA receptor antagonist MK 801 (0.25 mg/kg in saline, i.p.). Using overhead camera equipment

and Any-MAZE™ software, locomotor activity was recorded for 2.5 h post injection. Animals were carefully monitored and observed throughout testing.

2.4. Quantification of synapses

The number of spine synapses was calculated as published previously [6,11]. Vibratome sections (50 μsections (50 ions PFC and DG)) were cut and embedded in Durcupan (Electron Microscopy Sciences, Fort Washington, PA). Using the embedded sections, the volume of the sampling area was estimated using the Cavalieri Estimator module of the Stereo Investigator system (MicroBrightField Inc., Williston, VT) mounted on a Zeiss Axioplan 2 light microscope (Zeiss, Thornwood, NY). Thereafter, sampling regions were localized and approximately four 75-nm-thick consecutive ultrathin sections will be cut from each site. Digitized electron micrographs were taken for the physical dissector at a magnification of ×11,000 in a Tecnai 12 transmission electron microscope (FEI Co., Hillsboro, OR) furnished with a Hamamatsu HR/HR-B CCD camera system (Hamamatsu Photonics, Hamamatsu, Japan). The micrographs were taken in a blinded to treatment and genotype of individual animals. Spine synapses were counted according to the rules of the dissector technique, and the volumetric density of spine synapses (synapse/μm^3) was determined. The volumetric density was then multiplied by the volume of the sampling area to arrive at the total number of spine synapses (reported in billions, *i.e.* 10^9).

2.5. Auditory gating and gamma band power

Mice were anaesthetized with chloral hydrate injection (400 mg/kg, i.p.) and placed in stereotaxic frame (David Kopf Instruments, Tujunga, CA). The body temperature of mice was maintained at 37 °C by an isothermal heating pad. Craniotomy was performed above the hippocampus CA3 region and primary auditory cortex (pAC). Monopolar, stainless steel microelectrodes were placed into CA3 (2.2 mm posterior, 2.5 mm lateral, and 1.6 mm ventral from bregma) and pAC (3.0 mm posterior, 3.0 mm lateral, and 0.2 mm ventral from bregma) [12], and referenced to an indifferent electrode implanted over the cerebellum.

The paradigm of auditory stimulation was identical to the clinical protocol, consisting of two consecutive tone bursts of 10-msec duration at a frequency of 5 kHz with an inter-tone interval of 0.5 s. Tones were delivered through hollow ear bars. Auditory Evoked Potentials (AEPs) were determined by measuring the potential difference between the positive and the negative deflection 5–30 msec and 40–60 msec after stimulation (P20 and N40), respectively, as described previously [13]. For quantification, 60 sweeps were averaged, the amplitude was determined, and the ratio of the response after the second test stimulus (S2) and the first conditioning stimulus (S1) was calculated. This S2/S1 ratio was used as a measure of sensory (auditory) gating. The spontaneous field potential signals were subjected to Fast Fourier Transform; changes in power of gamma-band oscillations were monitored after digital band-pass filtering at 30–90 Hz. Neurophysiological data were captured and processed using Spike2 7.10 software package (Cambridge Electronic Design, Cambridge, UK).

2.6. Statistical analysis

Data was analyzed using FraphPad (San Diego, California). For comparison of the mean values between the two groups (UCP2 KO and WT) in the EPM, open field, gamma band power and auditory gating, baseline statistical evaluation was done using an unpaired, two-tailed student t-test. Repeated measures ANOVA was used to analyze data from the TST and locomotor response to MK 801. Data collected for the Y-maze and synaptic density were in non-normal distributions; these data sets were then analyzed with a non-parametric test, the Mann–Whitney U test. Analysis of the Lashley maze was done using a Log-rank Mantel test of the difference between Kaplan–Meier survival curves. The significance threshold was $p < 0.05$ for all conditions. Results are reported as mean ± SEM.

3. RESULTS

3.1. Elevated plus maze

In this measure of behavior, fewer entries into the open arms of the apparatus suggest higher levels of anxiety. KO mice demonstrated higher levels of anxiety when compared to WT animals: mean number of open arm entries, KO (5.33 ± 1.63); WT (15.50 ± 4.04); $t = 2.33$; $df = 11$, $p < 0.05$, KO ($n = 9$) and WT ($n = 10$), (Figure 1A).

3.2. Tail suspension test (TST)

In this measure, which is similar to the forced swim test, mice are placed in an inescapable but moderately stressful situation. Lack of escape related behavior is scored as immobility. Like the forced swim test, the TST is a test best validated for the evaluation of antidepressant efficacy of drugs, but also used to evaluate the effects of environmental, neurobiological, and genetic manipulations. Across the experiment findings show that KO animals spent a significantly greater percentage of time in an immobile position thought to be a measure of behavioral despair KO time immobile. Repeated measures ANOVA revealed the main effect of genetics (KO vs WT) $F(1, 105) = 9.22$, $p < 0.005$; main effect of time interval $F(4, 105) = 12.15$, $p < 0.0001$. There were no interaction effects of time and genetics, $F(4, 105) = 0.76$, $p = 0.55$ (Figure 1B).

3.3. Open field test

In this measure of baseline locomotion in a novel environment, there were no differences in UCP2 KO and WT animals after 5 min or 10 min of open field exploration; at 5 min, distance traveled, WT (14.82 ± 1.87); KO (12.25 ± 1.65), $t = 1.58$, $df = 17$, ($p < 0.15$); WT ($n = 10$) KO ($n = 9$); at 10 min, distance traveled, WT (10.89 ± 1.46); KO (9.14 ± 1.32), $t = 1.58$, $df = 17$, ($p < 0.15$) ($n = 10$) KO ($n = 9$) (Figure 1C).

3.4. Response to NMDA receptor blockade

UCP2 KO mice had increased locomotor response to NMDA receptor blockade produce by an i.p. injection of MK 801 (Figure 1D). Repeated measures ANOVA revealed a main effect of genetics $F(12, 143) = 38.08$, $p < 0.0001$; and a main effect of time interval $F(12, 143) = 5.70$, $p < 0.0001$. There were no interaction effects of time and genetics, $F(12, 143) = 1.16$, $p = 0.32$ (Figure 1B).

3.5. Y maze

The distance traveled in the novel arm, a proxy for exploratory behavior related to recognition of novelty differed significantly. KO mice traveled 2.57 ± 1.33 m while WT mice traveled 4.05 m ± 0.42 m) Results were in a non-normal distribution requiring a non-parametric analysis. (Mann–Whitney U prime = 9.0 KO ($n = 7$) WT ($n = 8$), $p < 0.05$ two-tailed) (Figure 2A) The time taken to discover the novel arm (latency to novel arm) was also significantly different across the groups KO (58 ± 30 s) and WT (5.2 ± 1.9 s). Again, distributions were non-normal requiring a non-parametric analysis (Mann–Whitney U prime = 11.0; KO ($n = 7$), WT ($n = 8$), $p < 0.05$ two-tailed (Figure 2B).

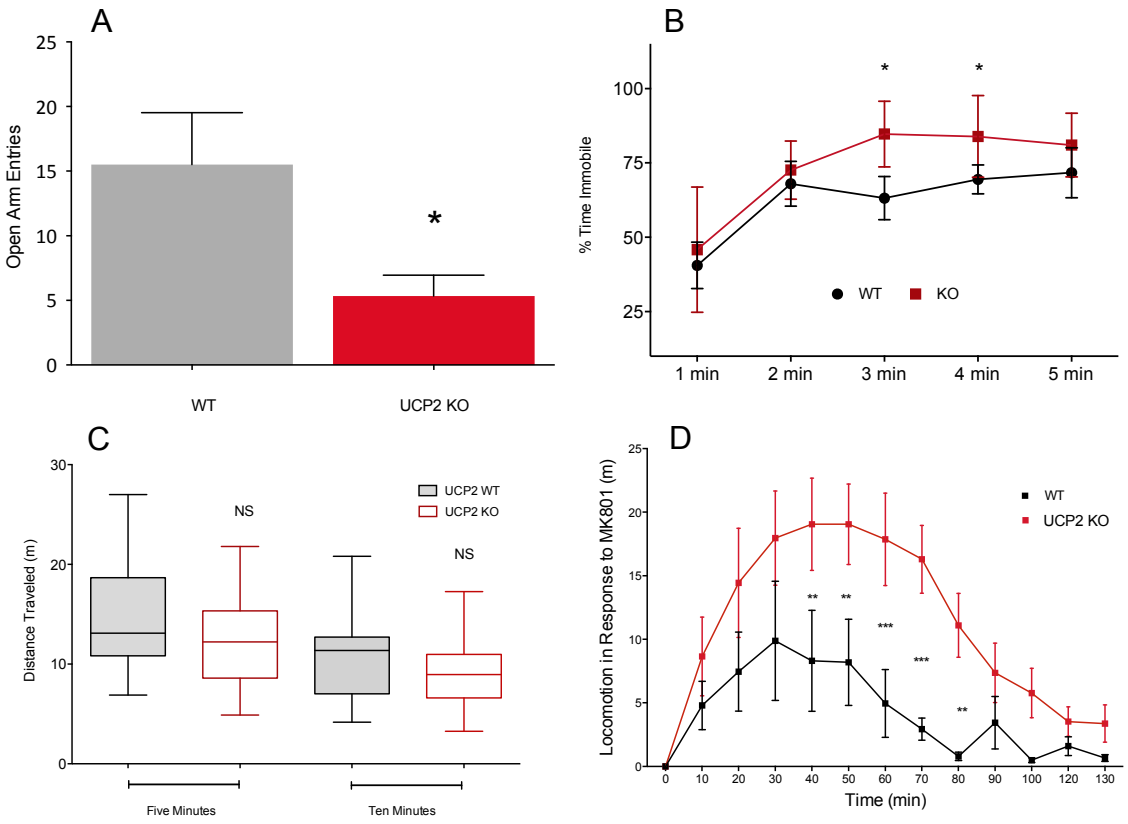

Figure 1: **A**. A behavioral measure of rodent anxiety, the elevated plus maze revealed behavioral dysregulation in KO mice (n = 9) compared to WT (n = 10) with fewer open arm entries among UCP2 KO mice, t-test *p < 0.05. **B**. The tail suspension test, a proxy behavioral assessment for depression and low motivation, revealed reduced motivation or a greater percentage of time spent immobile among UCP2 KO mice, ANOVA main effect of genetics (KO vs WT) F (1, 105) = 9.22, p < 0.005; main effect of time interval F (4, 105) = 12.15, p < 0.0001. **C**. In a measure of baseline locomotor activity we observed no differences in baseline motor activity between KO (n = 9) and WT (n = 10) mice, t-test, p > 0.05. **D**. Locomotor response (distance traveled) in response to NMDA receptor blockade (MK 801) revealed significantly greater activity with slower recovery to baseline movement among KO mice (n = 6) when compared to WT mice (n = 8), main independent effects of genetics and time, p < 0.0001. Results for behavioral testing (Figure 1A–D) are expressed as the mean ± S.E.M.

3.6. Lashley maze

On the Lashley maze, a measure of learning and spatial memory, UCP2 KO mice demonstrated significant delays in learning relative to UCP2 WT (Figure 2C) comparison of Kaplan–Meier survival curves of mean days required to achieve learning criterion, Log-rank Mantel test, $\chi^2 = 4.99$, df = 1, ($p < 0.03$).

3.7. Electron microscopy

Synaptic density: EM analysis of synapses in dentate gyrus revealed increased percentage of synaptic density in KO's relative to WT's (Figure 2D–F, Mann–Whitney, $p < 0.001$).

3.8. Neurophysiological measures

Results demonstrated enhanced baseline gamma band power and impaired auditory gating in the auditory cortex of UCP2 KO mice (Figure 3A, B). Absolute gamma band power in the primary auditory cortex is increased in UCP2 KO mice compared to their age matched WT counterparts (Figure 3A). WT (n = 5) $6.01 \times 10^{-5} \pm 3.23 \times 10^{-6}$; KO (n = 5) $1.28 \times 10^{-4} \pm 2.045 \times 10^{-5}$; (*$p < 0.01$). Auditory gating in the auditory cortex was altered in UCP2 KO animals compared to controls (Figure 3B). WT (n = 5) 0.70 ± 0.02 and KO (n = 5) 1.1 ± 0.07 (*$p < 0.01$). Significantly enhanced gamma band power was also observed in the CA3 region of the hippocampus of UCP2 KO mice compared to WT mice, WT (n = 5) $2.91 \times 10^{-4} \pm 1.92 \times 10^{-5}$; KO (n = 5) $4.28 \times 10^{-4} \pm 4.41 \times 10^{-5}$ (*$p < 0.02$) (Figure 3C). There were no differences in auditory gating between the UCP2 KO and WT groups in the hippocampus CA3 region, WT (n = 5) 0.63 ± 0.11 and KO (n = 5) 0.72 ± 0.13; (p = 0.62) (Figure 3D).

4. DISCUSSION

Using an animal model of mitochondrial dysfunction, UCP2 KO, we have explored responses to NMDA receptor blockade, synaptic density, auditory gating and gamma power. These measures and markers relevant to the pathophysiology of mental illnesses, revealed a significant vulnerability in animals with UCP2 deficiency. In a measure of rodent anxiety, the elevated plus maze, UCP2 KO mice demonstrated significantly greater anxiety. We have hypothesized that heightened anxiety response in KO animals is linked to NMDA receptor dysfunction. In other animal models of aspects of psychopathology, NMDA receptor blockade alleviates anxiety and fear. We have also shown in two tests of hippocampal-based behavior—the Lashley maze and the Y maze—deficits in procedural memory and spatial cognition. We have also shown increased synaptic density in the dentate gyrus of UCP2 KO mice. The increase in synaptic density may reflect dysregulation in formation, pruning and synaptic maintenance considered to contribute to mental illness and contingent on mitochondrial support [14,15].

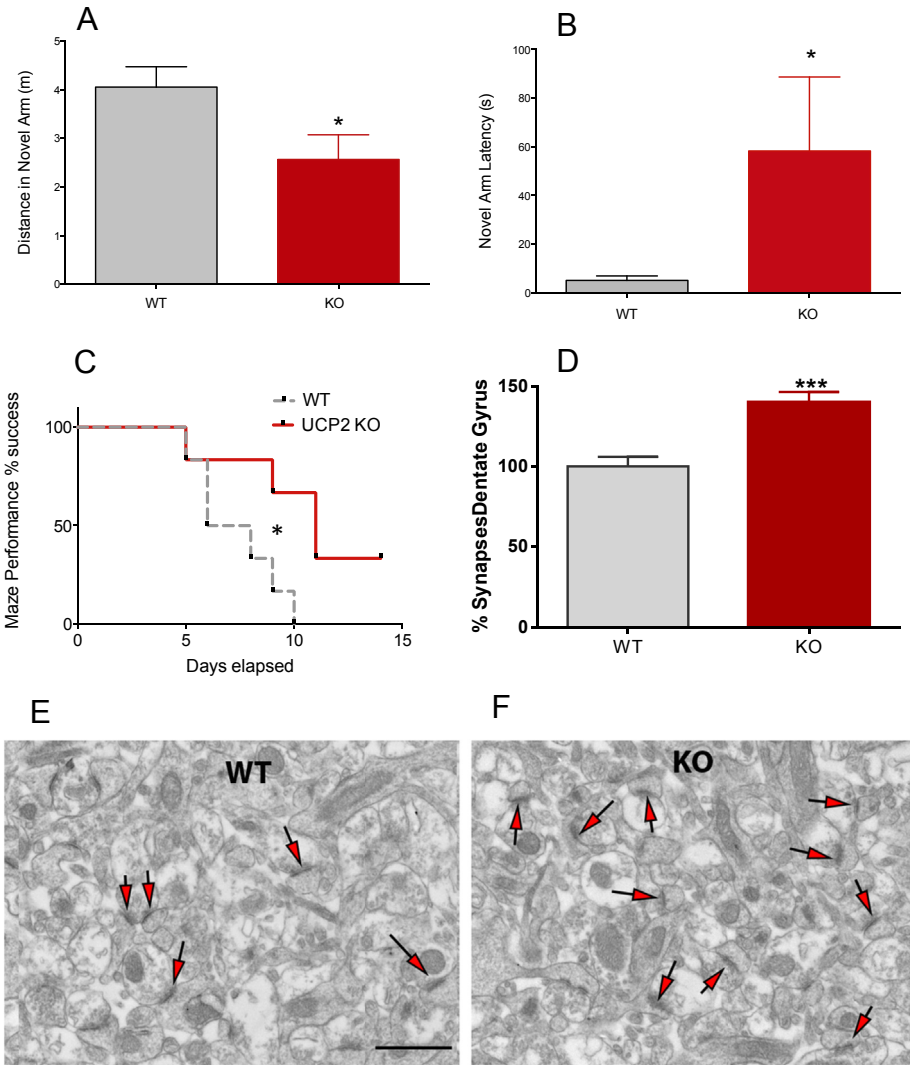

Figure 2: **A**—**B**. The Y-maze revealed differences in procedural and spatial memory. When compared to WT mice (n = 8) KO mice (n = 7), spent less time exploring the novel arm (distance traveled in the novel arm) and took longer to identify the novel arm (novel arm latency), t-test, *p < 0.05. Results are expressed as the mean ± S.E.M. **C**. Kaplan—Meier survival curve is used to express differences between KO's (n = 6) and WT's (n = 6) mice in the number of testing days required to reach a pre-established learning criterion on the Lashley maze, Log-rank, Mantel—Cox test, *p < 0.05. **D**. Bar graphs depicting a quantitative analysis of spine synapse number in dentate gyrus of hippocampus. *p < 0.05. **E**, **F**: Representative electron micrographs showing spine synapses in the dentate gyrus of wild type (wt) and UCP2 KO (KO) mice. Bar scale represents 1 um.

Impaired NMDA receptor function likely accounts for significant deficits in cognition as well as negative and positive symptoms among the mentally ill. Most of these abnormalities can be elicited in healthy subjects with NMDA receptor antagonists, such as ketamine, which is known to induce cognitive impairments as well as positive and negative symptoms resembling those displayed by schizophrenic patients [3]. In rodent models, NMDA receptor blockade, via MK 801 in this case, elicits a characteristic motor syndrome of increased locomotion, ataxia and stereotypy. UCP2 KO animals were significantly more vulnerable to NMDA receptor blockade as measured by significant increases in locomotion and stereotypy (data not shown). Importantly, we did not see differences in locomotion in treatment naïve animals in open field tests measuring distance traveled. This finding indicates that the response to MK 801 is not driven by baseline differences in motor activity between WT and KO animals.

Related to these findings, increasing attention has been paid to NMDA receptor mediated biomarkers of mental illness including abnormal brain oscillations and information processing. In experimental animals, systemic administration of NMDA receptor antagonists elicits aberrant gamma band oscillations and impaired auditory gating—considered a potential marker of schizophrenia [16]. The present *in vivo* electrophysiological findings related to gamma oscillations and auditory gating indicate an NMDA receptor dysfunction in UCP2 KO mice. Together these behavioral, anatomic, and physiological findings demonstrate the importance of animal models that facilitate understanding of the role of bioenergetics and mitochondrial function in mental illness. An important limitation in the research presented here relates to the use of a whole body UCP2 knockout. Based on these studies then, it is not possible to rule out the importance of systemic events in the development of the phenotype. Further studies utilizing brain region specific UCP2 ablation are needed to understand the connection between energetics and the higher brain functions examined here.

The brain is a remarkably avid consumer of energy, representing 2% of the body weight and accounting for greater than 20% of oxygen

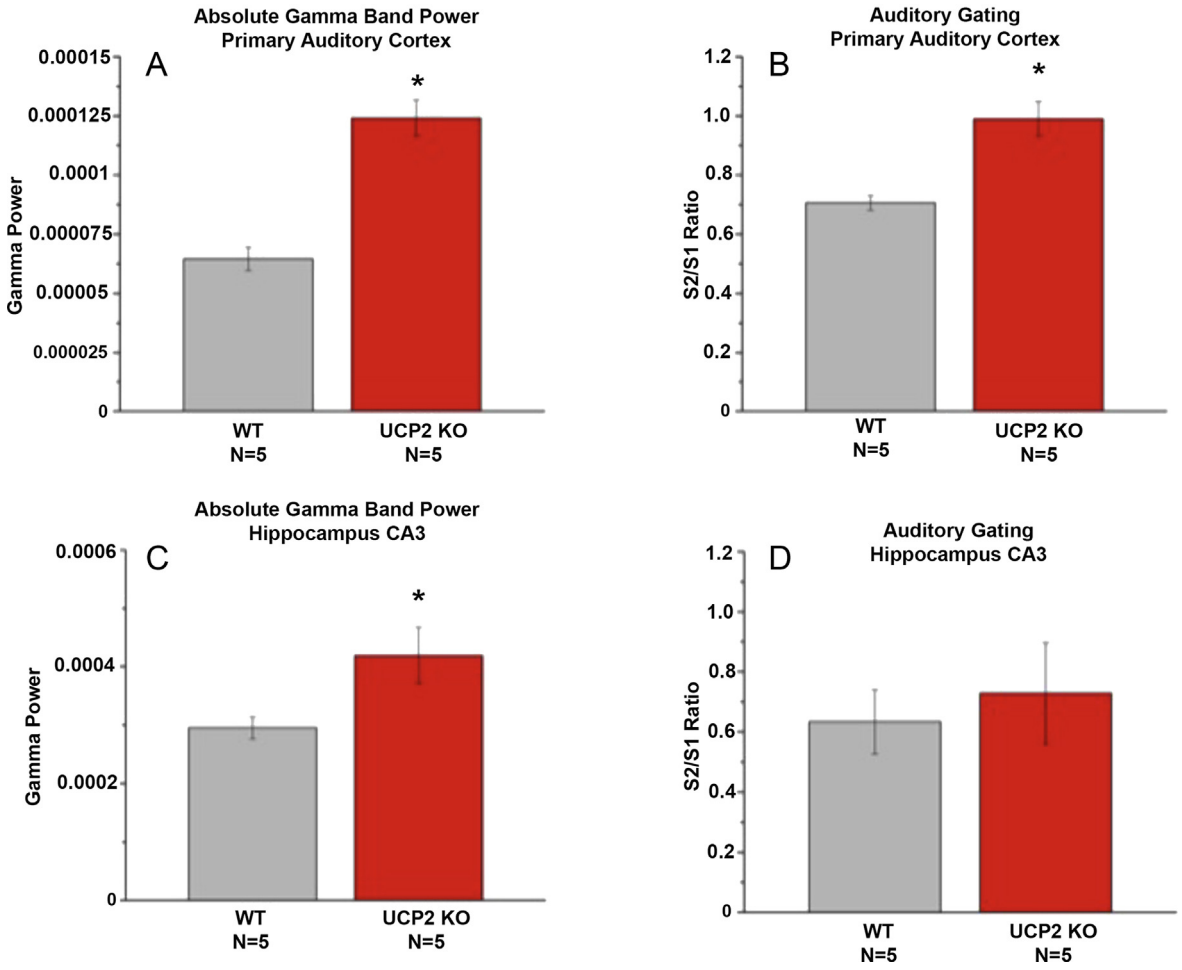

Figure 3: Neurophysiological measures to assess the functional integrity of neuronal circuits. **A**, **B**. Gamma-band power and auditory gating reported in the primary auditory cortex. **C, D**. Gamma-band power and auditory gating reported in hippocampus CA3 region. KO ($n = 5$) and WT ($n = 5$), t-test, *$p < 0.05$.

consumption. These metabolic requirements are associated significantly with glutamate signaling—80% of neurons are excitatory and greater than 90% of synapses release glutamate. Studies have shown that 80% of energy utilized by the brain supports events related to neurotransmission and cycling of neurotransmitters GABA and glutamate [17]. Further, *in situ* work has shown that glutamate-driven NMDA receptor activation consumes the full respiratory capacity of mitochondria, 80% attributable to increases in ATP demand [18].

Research has shown that glutamate and GABA are increasingly implicated in a wide variety of neuropsychiatric illnesses. NMDA blockade, with ketamine or MK-801, leads to a surge in glutamate that mimics a range of psychiatric symptoms, as well as longer-lasting circuit changes that can produce an anti-depressant effect. Disruption of mitochondria is likely to have an early, disproportionate effect on glutamate and GABA production and homeostasis. Our work suggests that mitochondrial dysregulation, which may be the result of altered systemic metabolism, may be an important contributor in the etiology of psychiatric disease.

FUNDING SOURCES

GH supported by the APA-Pfizer M.D., Ph.D. Research Fellowship from the American Psychiatric Association, NARSAD Young Investigator Award (2015), and a Schizophrenia Research Fellowship supported by the Veteran's Administration and the Yale Department of Psychiatry.

AUTHOR CONTRIBUTIONS

G.H. performed behavioral studies and NMDA challenge test as well as shared responsibility for experimental design. G.H. wrote the manuscript, except for portions indicated below. M.W. performed the tail suspension test. D.N. performed the neurophysiological studies, gamma band power and auditory gating. M.H. designed the neurophysiological studies and wrote the methods and results related to these measures. L.V. did the quantification of neural synapses. T.H. was involved in experimental design, data analysis, and interpretation.

CONFLICT OF INTEREST

The authors declare no competing financial interests.

REFERENCES

[1] Manji, H., Kato, T., Di Prospero, N.A., Ness, S., Beal, M.F., Krams, M., et al., 2012. Impaired mitochondrial function in psychiatric disorders. Nature Reviews. Neuroscience 13(5):293–307.

[2] Fattal, O., Link, J., Quinn, K., Cohen, B.H., Franco, K., 2007. Psychiatric comorbidity in 36 adults with mitochondrial cytopathies. CNS Spectrums 12(6):429—438.
[3] Abdallah, C.G., Jiang, L., De Feyter, H.M., Fasula, M., Krystal, J.H., Rothman, D.L., et al., 2014. Glutamate metabolism in major depressive disorder. The American Journal of Psychiatry 171(12):1320—1327.
[4] Sans, N., Petralia, R.S., Wang, Y.X., Blahos 2nd, J., Hell, J.W., Wenthold, R.J., 2000. A developmental change in NMDA receptor-associated proteins at hippocampal synapses. The Journal of Neuroscience 20(3):1260—1271.
[5] Gigante, A.D., Andreazza, A.C., Lafer, B., Yatham, L.N., Beasley, C.L., Young, L.T., 2011. Decreased mRNA expression of uncoupling protein 2, a mitochondrial proton transporter, in post-mortem prefrontal cortex from patients with bipolar disorder and schizophrenia. Neuroscience Letters 505(1):47—51.
[6] Dietrich, M.O., Andrews, Z.B., Horvath, T.L., 2008. Exercise-induced synaptogenesis in the hippocampus is dependent on UCP2-regulated mitochondrial adaptation. The Journal of Neuroscience 28(42):10766—10771.
[7] Andrews, Z.B., Diano, S., Horvath, T.L., 2005. Mitochondrial uncoupling proteins in the CNS: in support of function and survival. Nature Reviews. Neuroscience 6(11):829—840.
[8] Denenberg, V.H., Sherman, G.F., Schrott, L.M., Rosen, G.D., Galaburda, A.M., 1991. Spatial learning, discrimination learning, paw preference and neocortical ectopias in two autoimmune strains of mice. Brain Research 562(1):98—104.
[9] Bressler, A., Blizard, D., Andrews, A., 2010. Low-stress route learning using the Lashley III maze in mice. Journal of Visualized Experiments(39).
[10] Dellu, F., Mayo, W., Cherkaoui, J., Le Moal, M., Simon, H., 1992. A two-trial memory task with automated recording: study in young and aged rats. Brain Research 588(1):132—139.
[11] Diano, S., Farr, S.A., Benoit, S.C., McNay, E.C., da Silva, I., Horvath, B., et al., 2006. Ghrelin controls hippocampal spine synapse density and memory performance. Nature Neuroscience 9(3):381—388.
[12] Paxinos, G., Franklin, K., 2007. The mouse brain in stereotaxic coordinates. , NY, NY: Academic Press.
[13] Hajos, M., Hurst, R.S., Hoffmann, W.E., Krause, M., Wall, T.M., Higdon, N.R., et al., 2005. The selective alpha7 nicotinic acetylcholine receptor agonist PNU-282987 [N-[(3R)-1-Azabicyclo[2.2.2]oct-3-yl]-4-chlorobenzamide hydrochloride] enhances GABAergic synaptic activity in brain slices and restores auditory gating deficits in anesthetized rats. The Journal of Pharmacology and Experimental Therapeutics 312(3):1213—1222.
[14] Kang, H.J., Voleti, B., Hajszan, T., Rajkowska, G., Stockmeier, C., Licznerski, P., et al., 2012. Decreased expression of synapse-related genes and loss of synapses in major depressive disorder. Nature Medicine 18(9):1413—1417.
[15] Glausier, J.R., Lewis, D.A., 2013. Dendritic spine pathology in schizophrenia. Neuroscience 251:90—107.
[16] Kocsis, B., Brown, R.E., McCarley, R.W., Hajos, M., 2013. Impact of ketamine on neuronal network dynamics: translational modeling of schizophrenia-relevant deficits. CNS Neuroscience & Therapeutics 19(6):437—447.
[17] Shulman, R.G., Rothman, D.L., Behar, K.L., Hyder, F., 2004. Energetic basis of brain activity: implications for neuroimaging. Trends in Neurosciences 27(8):489—495.
[18] Yadava, N., Nicholls, D.G., 2007. Spare respiratory capacity rather than oxidative stress regulates glutamate excitotoxicity after partial respiratory inhibition of mitochondrial complex I with rotenone. The Journal of Neuroscience 27(27):7310—7317.

